Integrated Nanophotonic Control of Thermal Bimorph Microactuators*

Maziar P. Nezhad[1]

***Abstract*— A new type of thermal bimorph microactuator is presented, in which energy delivery to the actuator is achieved through an integrated nanophotonics approach. This approach has been adopted from existing photonic device and optical communications technology. The microactuators are fabricated on a silicon nitride platform using a silicon nitride/aluminum bimorph structure. Integrated nanophotonic building blocks, such as waveguides, tapers and grating couplers are designed and fabricated using photonic design and nanofabrication tools. During operation, laser light from a telecommunications laser source at milliwatt levels is focused onto the device and is captured by the grating coupler. The captured light is routed on the surface of the microstructure and delivered to the bimorph limbs by the waveguides and subsequently converted to heat using chromium optical absorbers integrated onto the waveguides. To provide additional mechanical flexibility and increased bending range, solid rib waveguides are replaced in parts by arrays of etched ridges which are periodically spaced at a fraction of the laser wavelength. These 1-D photonic crystals act as flexible subwavelength grating waveguides. As an added feature, the grating couplers are implemented as 2D arrays of etched holes, enabling polarization-based beam separation on the device, thus enabling control of different limbs through polarization switching at the laser source. In addition to in situ characterization, the microstructures are also transferred to an optical fiber tip which delivers laser light to the device while also providing a useful means for packaging and using the microactuators.**

I. INTRODUCTION

Microactuators and microlimbs are key components for the practical realization of microrobots. Microcantilevers in the form of bimorphs are commonly used for this purpose [1]. Such structures are also important in the MEMS domain as sensors and actuators [2]. Among the various types of such microactuators, thermal bimorphs are among the most straightforward to implement, due to their relative ease of fabrication and large range of motion.

As with any other actuator, energy must be delivered in an appropriate manner to the device to enable correct operation. This can be through electrical [3], optical [4] or other methods. Optical energy delivery possesses attractive characteristics, including wireless delivery and good spatial selectivity. Bimorph optically-driven actuators have been used to realize different microrobotic devices, such as terrestrial walking microrobots [5]. Through the use of spatial positioning of a free-space light beam (e.g., a laser beam controlled with a galvoscanner) it is possible to to select individual limbs or sections of limbs to induce a gait sequence. Simultaneous multi-limb control can be approximated through fast spatial switching between the robot limbs, however this does not utilize all that is possible with light. Light possesses features such as polarization and wavelength, which, if leveraged properly, can provide additional means of microlimb actuation and control. Alongside this, advances in integrated nanophotonics over the past three decades have yielded an extensive toolbox for control and guidance of light on a photonic chip using planar optical waveguides. To date, most of this research has been geared towards applications in telecommunications, sensing and imaging. The work presented here demonstrates an example of how integrated nanophotonics can be used to develop new approaches for optical control of microrobotic actuators.

II. MATERIAL CHOICES FOR THERMAL BIMORPHS INTEGRATED WITH NANOPHOTONIC WAVEGUIDES

The core idea in this work is to integrate nanophotonic waveguides with thermal bimorphs to be able to selectively induce motion in one (or several) devices in a controllable manner, using properties of the light beam. Fig. 1(a) depicts an initial starting design for such a device. The waveguide guides light along the length of the bimorph to an absorbing section, which converts this light to heat, resulting in bending of the bimorph. Since our aim is to create bimorph actuators with an appreciable range of motion, we need to choose the bimorph materials to have very different thermal expansion coefficients. On the other hand, since we are aiming to integrate nanophotonic waveguides into the same structure, the chosen materials need to be compatible with microfabrication and nanofabrication processes and also be able to guide or absorb light, as needed. Among suitable materials, aluminum has one of the highest thermal expansion coefficients (23.1 ppm/°C) and can be deposited using a variety of thin film deposition techniques (e.g., thermal or e-beam deposition). At the other end of the scale, silicon and silicon nitride have very small thermal expansion coefficients (2.56 ppm/°C and 3.27 ppm/°C, respectively) and have the necessary transparency and high refractive index needed for high quality optical waveguides. Between the two, we choose silicon nitride, since low stress membranes can be grown and isolated with relative ease (e.g., by LPCVD growth on a silicon substrate and subsequent KOH etching of the underlying substrate). The absorbing section needs to provide sufficient optical loss to absorb all or most of the incoming light over the length of the bimorph. While the inclusion of an aluminum layer on top of the waveguide

*This work was supported through a UKRI/EPSRC Innovation Fellowship (EP/S001425/1) and the North of England Robotics Innovation Centre (NERIC)

[1]Maziar P. Nezhad is with the School of Science, Engineering and Environment, University of Salford, M5 4WT, United Kingdom m.p.nezhad@salford.ac.uk

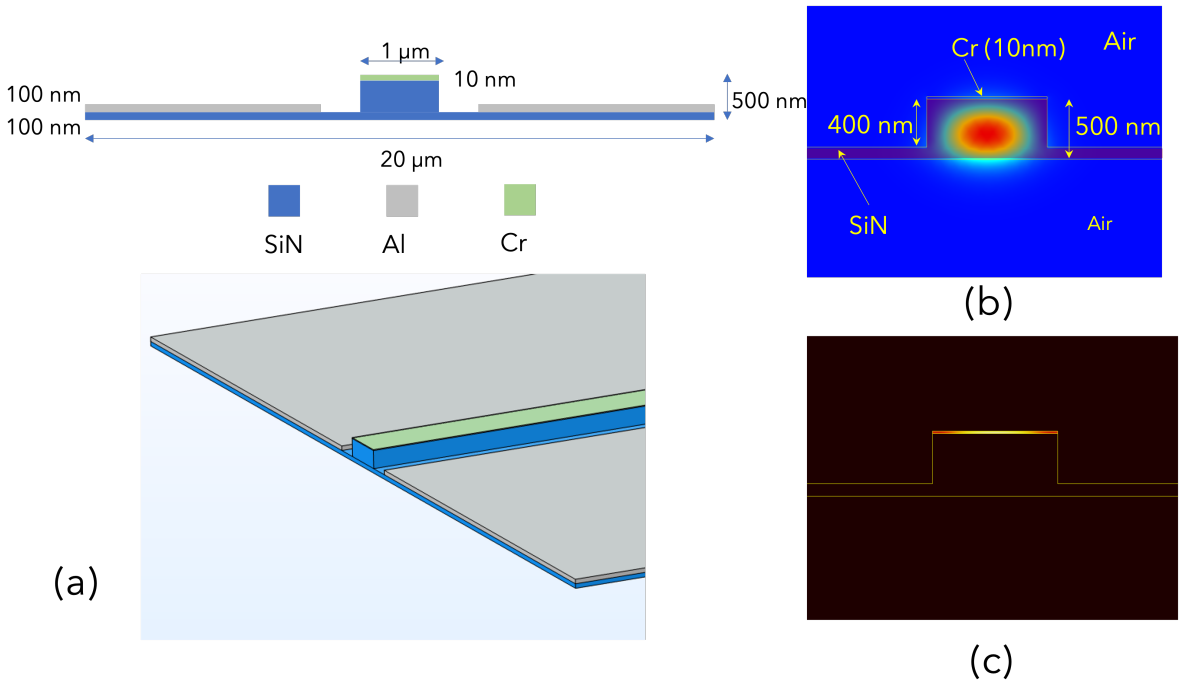

Fig. 1. (a) Structure and cross section of a waveguide-driven absorbing section of an Al/SiN bimorph. The absorption of the TE waveguide mode (b) is shown in the heatmap (c).

will result in some light being absorbed, calculations show that complete absorption will require a comparatively long absorption length. Instead, here a thin layer of chromium is used, which will provide a much higher absorption per unit length, which translates to localized heat generation.

III. Waveguide Design

Most planar photonic waveguides are fabricated by plasma etching a masked substrate in a reactive chemistry (e.g., fluorine-based for silicon nitride), resulting in nearly vertical waveguide sidewalls and a rectangular waveguide core structure, surrounded by a lower refractive index cladding. For many reasons it is preferable to design the waveguide to be single mode (i.e. have only one mode in each of the horizontal and vertical directions). Since the bulk of integrated photonic devices and test equipment are targeted to near-infrared telecommunication bands the designs here are centered around a wavelength of 1550 nm. One exemplar design, obtained through finite element eigenmode calculation (COMSOL), is the rib waveguide shown in Fig. 1(b), with the power distribution in the waveguide superimposed on the core. The mode polarization is transverse electric (TE) with the electric field predominantly pointing in the horizontal direction. This design can be readily by etching a 500 nm suspended silicon nitride membrane, providing both a 400 nm guiding core and a 100 nm base for the bimorph.

Fig. 1(b) also depicts the absorbing section of the waveguide, which consists of a thin (10nm) Cr layer on the top surface of the waveguide ridge. Such a distribution of chromium is readily attained through a directional thin film deposition method such as thermal or e-beam deposition. Calculation of the complex eigenmode of this structure yields a mode absorption coefficent of 0.2/µm, corresponding to $1/e$ absorption length of about 5 µm. Fig 1(c) shows the absorption map of the optical mode in the chromium layer.

IV. Bimorph Design

The first step in designing the bimorph is to place an optimal thickness of aluminum to create maximal bending. Thermomechanical finite element design (COMSOL) yields an optimal aluminum thickness of about 100 nm for a 100 nm silicon nitride layer. The calculated displacement over 100 °C temperature change and the resultant bending of a 100 µm long SiN/Al(100 nm/100 nm) bimorph is shown in Fig. 2(a), which seems quite acceptable. However, combining this design with the 400 nm thick rib waveguide design proposed in the previous section poses a major problem. As shown in Fig 2(b), the range of motion over the same temperature change is severely reduced. This is mainly due to the presence of the relatively thick 500 nm waveguide core, since it considerably stiffens the structure, thus inhibiting the achievable range of motion. This can also be seen in the displacement curve of Fig 2(c) At first glance this issue seems insurmountable, since the relatively thick SiN rib is needed for light confinement and guidance. However, as the next section will demonstrate, a nano-engineered waveguide

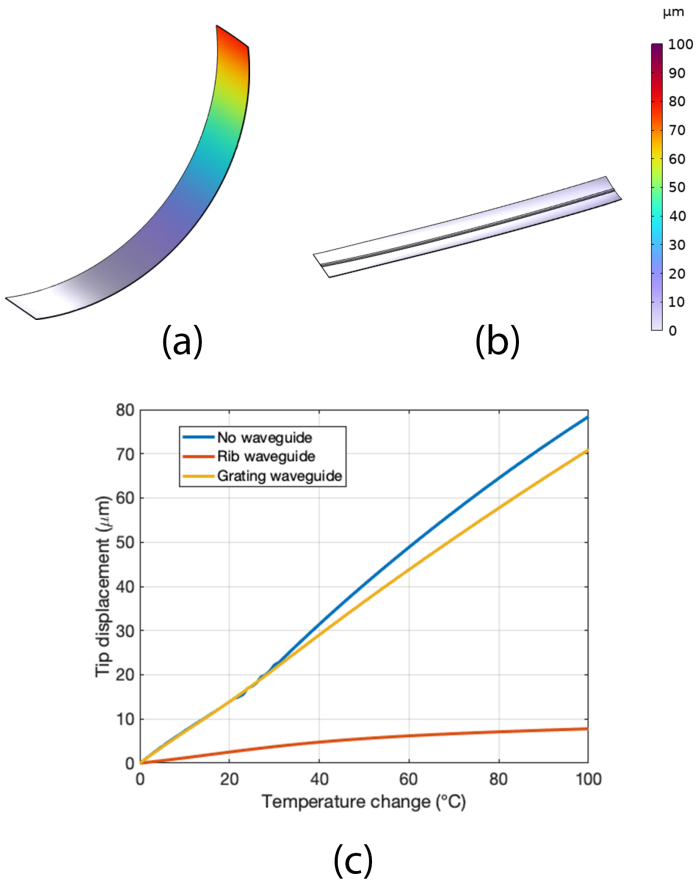

Fig. 2. (a) A SiN/Al bimorph cantilever bent under 100°C temperature change. The cantilever measures 100 μm by 20 μm and the SiN and Al thicknesses are 100 nm each. (b) A bimorph cantilever with the same dimensions undergoing the same temperature change, but with a 1000 nm x 400 nm thick rib 'spine' included along the main axis, following the design shown in Fig. 1(a). (c) Plot of tip displacement vs. temperature for the structures in (a) and (b), (the tip displacement of a bimorph with a disconnected subwavelength grating waveguide is also shown for comparison).

can provide an effective solution for solving this problem.

V. Subwavelength grating waveguides

The simplest form of waveguide is a high index core surrounded by a low index cladding, with continuous translational symmetry along the length of the waveguide. Such a structure will guide a waveguide eigenmode, without any change of the mode shape. Any disturbance in the shape of the waveguide (e.g. a small perturbation of the core) will result in some amount of light becoming scattered into different directions. However, if these disturbances are arranged in a periodic fashion, light will scatter into distinct directions and modes. Such a periodically structured waveguide is termed a grating waveguide (the guided wave counterpart of a diffraction grating) or alternatively a 1-D photonic crystal (Fig. 3(a)). Such waveguides are commonly used in integrated photonics as Bragg filters and Bragg mirrors [6]. However, if the period of the grating is 'much smaller' than the wavelength then all the scattered modes disappear and light will propagate in the waveguide without loss. A periodic waveguide operating under such conditions is termed a 'subwavelength grating waveguide'[6] (Fig. 3(c)). Interestingly, if the waveguide core is removed, the remaining periodic array of isolated ridges (Fig. 3(b)) will also act as a lossless waveguide, as long as the conditions for sub-wavelength operation are maintained. This last scenario is important in the context of the waveguide-actuated bimorph. Substituting the solid waveguide ridge with a sub-wavelength sequence of disconnected nanoscale ridges will create a much more mechanically flexible structure, while still allowing for light to be guided along the length of the bimorph. Depositing a thin layer of chromium on and between the grating ridges will convert light into heat, as before. The design process to create a subwavelength grating waveguide is performed by solving for the Bloch mode of a unit cell (one period) of the periodic structure. The Bloch mode solutions are calculated using a finite element eigenmode solver (COMSOL), which results in a grating period of 430 nm for this particular design. Simulation of the thermomechanical bending of this structure shows that it is on par with the original bimorph (see Fig. 2(c)).

VI. Coupling light into the waveguides

In order to correctly actuate the bimorphs, we need to couple light from a free-space laser beam into the waveguides. This cannot be done by shining the light

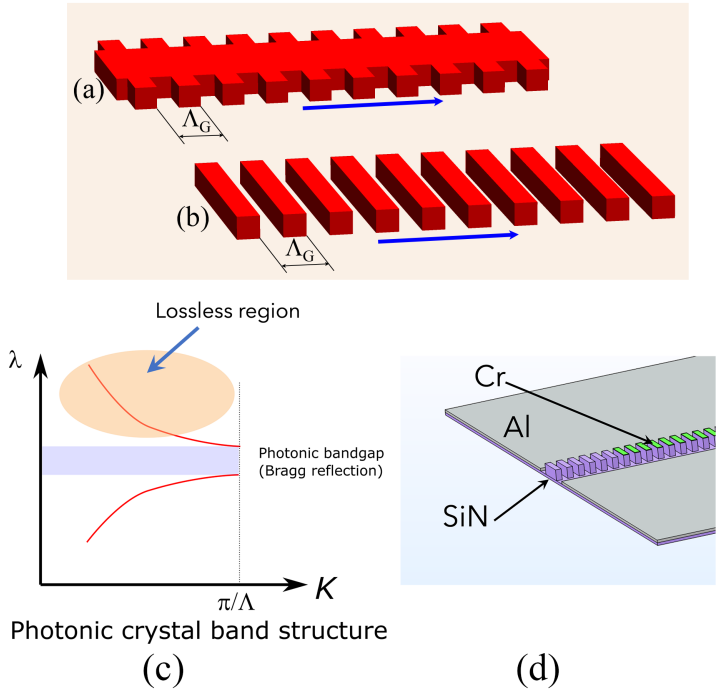

Fig. 3. (a) Structure of a side-wall modulated grating waveguide (also known as a 1-D photonic waveguide). (b) The grating waveguide with the spine removed, resulting in a sequence of disconnected blocks. (c) Depiction of the first bandgap of the 1-D photonic waveguide. In the region above the bandgap the wavelength is long enough to propagate in the waveguide without any scattering losses. (d) The bimorph structure with a discrete subwavelength grating waveguide instead of the solid waveguide of Fig. 1(a). The flexibility of this structure is very close to the bimorph without a waveguide, as shown in Fig. 2(c).

laterally onto the waveguide, since the intention is excite a guided mode. Rather, a diffraction grating with the correct period and Bloch mode index is needed to provide the necessary coupling. Such a device is termed a grating coupler in integrated photonics nomenclature [7] . A 1-D array of etched lines will couple a normally incident light beam into left and right travelling beams (propagating perpendicularly to the grating ridges), as long as the light is polarized such that the electric field is parallel to the grating lines. To couple light of both polarizations, one can instead use a 2D array of holes. In this case, the light will split into two of counter-propagating beam pairs, with each pair carrying the corresponding polarization. Such a device is used as a polarization diversity coupler in telecommunications [8]. As will be discussed, this allows us to control individual limb pairs through polarization switching.

VII. Fabrication

Based on the principles mentioned above, bimorph microactuators were designed and fabricated on 500 nm LPCVD nitride membranes. The membranes were grown on silicon substrates and undercut in hot KOH. Waveguide and grating structures were patterned on the membrane using electron beam lithography and partially etched into the membrane with CHF_3/O_2 plasma. Chromium and aluminum were e-beam deposited, patterned with optical laser lithography and wet etched. Finally, the bimorphs were patterned with a final laser lithography and released through a final plasma etch step. Fig. 4 shows SEM and optical microscope images of the fabricated devices.

VIII. Characterization

Two sets of devices were designed for this experiment. One group was designed for in-situ characterization on the chip. These devices were actuated using light from a multi-port tunable C-band telecom laser. The outputs of two laser ports were sent into a polarization maintaining fiber (having a 128 μm diameter and a 9 μm core). Each laser was sent into a separate optical axis of the fibre using a polarization multiplexer and fibre rotator. The laser outputs were modulated with MEMS optical switches placed at each laser output. The lasers were set to the vicinity of 1550 nm and tuned slightly to maximise the bimorph deflection. Each laser output was set to 20 mW. The polarization maintaining fiber output facet was brought to approximately 100 μm above the microstructure and its core was aligned to the grating coupler for maximum cantilever displacement. The fast and slow axes of the fiber were also aligned to the axes of the grating coupler.The first section of the accompanying video clip shows the result of switching the outputs of the lasers to alternately excite each pair of cantilevers, which demonstrates polarization-based selection and control of the cantilevers. Also, interestingly, in the video there is some evidence of instability and thermal limit cycle behaviour in the limbs, which brings up the possibility of creating self-sustained oscillatory action in the limbs under appropriate

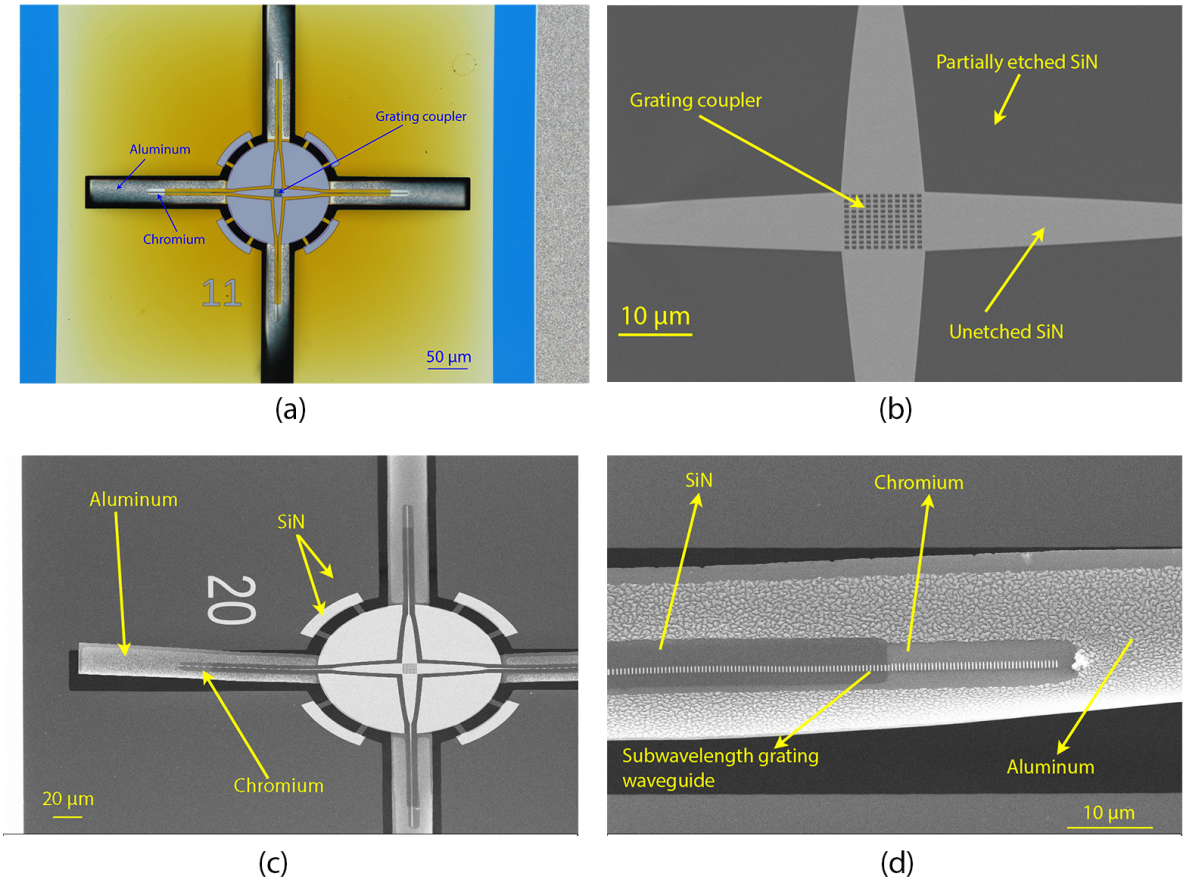

Fig. 4. (a) Optical microscope image of a 4-limbed laser actuated microstructure. (b) A 2D grating coupler partially etched into SiN. Light is incident normal to the plane of the coupler and will be diffracted into the left/right or up/down waveguide taper pairs, depending on the polarization. The period of the grating coupler is 930 nm. (c) SEM image of another microstructure from the same chip. (d) Close-up of an SiN/Al bimorph limb, showing the aluminum and chromium layers on and surrounding the partially etched SiN subwavelength grating waveguide.

conditions.

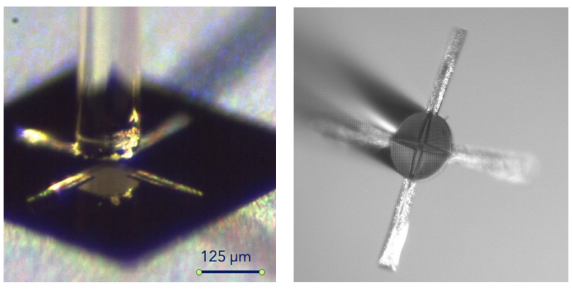

Fig. 5. (a) A 4-limbed microstructure under in situ testing. The optical fiber is positioned approximately 100 µm above the device. (b) A 4-limbed microstructure mounted on the tip of a polarization maintaining fiber. In both cases the core of the fiber is aligned to the grating coupler for maximum light coupling.

The second group of microstructures were designed for fiber-tip integration. The disc shape of the devices (Fig. 4(a) and 4(c)) was designed to match the diameter of the optical fiber. After the final fabrication step, the microstructures were transferred to the cleaved facet of the polarization-maintaining fiber tip and fixed in place with UV-curable epoxy (Fig. 5(b)). Before the curing step, the fiber core and fiber axes were aligned to the grating coupler for maximal deflection. Since the grating coupler efficiency was lower in this case, only one laser port was used in conjunction with an erbium doped fiber amplifier (EDFA), in order to provide more power at the fiber output. The light output of the EDFA was set to 200 mW and the light was controlled using the MEMS switch as before. As shown in the second part of the video, only the pair of limbs corresponding to the incoming beam polarization are moving, which demonstrates that optical power is being delivered to the limbs and that polarization separation is occurring on the device as intended. Further characterization work is under way to quantify the device movement range and power efficiency, which will be reported in future publications.

IX. Conclusion

It has been shown that techniques used in integrated nanophotonics can be used to actuate and control microrobotic structures with potentially higher finesse and sophistication compared to simple spatial beam

manipulation. More advanced control paradigms based on other properties of light such as wavelength are also possible. Improved designs, such as more efficient grating couplers, can substantially reduce the power budget needed to operate these devices, especially in the case of fiber mounted devices. Efficent fiber tip integration of microrobotic devices, together with new methods of nanophotonic control may provide a promising future for developing new microrobotic surgical and manipulation tools.

REFERENCES

[1] O. J. Sul et al., 'Thermally actuated untethered impact-driven locomotive microdevices, Applied Physics Letters, vol. 89, no. 20, p. 203512, 2006.

[2] C. R. Knick, et al., 'High frequency, low power, electrically actuated shape memory alloy MEMS bimorph thermal actuators,' J. of Micromechanics and Microengineering, vol. 29, iss. 7, 2019.

[3] R. J. Wood, et al., 'Optimal energy density piezoelectric bending actuators,' Sensors and Actuators A-Physical, vol. 119, iss. 2, pp. 476-488, 2005.

[4] S. R. Manalis et al., 'Two-dimensional micromechanical bimorph arrays for detection of thermal radiation,' Applied Physics Letters, vol. 70, iss. 24, pp. 3311-3313, 1997.

[5] M. Han et al., 'Submillimeter-scale multimaterial terrestrial robots', Science Robotics, vol. 7, iss. 66, eabn602, 2022.

[6] R. Halir et al., 'Waveguide sub-wavelength structures: a review of principles and applications', Laser Photonics Rev, 9, No. 1, pp. 25-49, 2015.

[7] L. Chrostowski and M. Hochberg, Silicon Photonics Design, Cambridge University Press, ch.5, 2015.

[8] D. Taillaert et al., 'A compact two-dimensional grating coupler used as a polarization splitter,' IEEE Photonics Technology Letters, vol. 15, iss. 9, pp. 1249-1251, 2003.